Voltage Harmonic Compensation of a Microgrid Operating in Islanded and Grid-Connected Modes

Savaghebi, Mehdi; Jalilian, Alireza ; Vasquez, Juan C. ; Guerrero, Josep M.; Lee, Tzung-Lin

Published in:
Proceedings of the 19th Iranian Conference on Electrical Engineering, ICEE 2011

Publication date:
2011

Document Version
Early version, also known as pre-print

Voltage Harmonic Compensation of a Microgrid Operating in Islanded and Grid-Connected Modes

Mehdi Savaghebi[1], Alireza Jalilian[1], Juan C. Vasquez[2], Josep M. Guerrero[2,3], and Tzung-Lin Lee[4]

1- Center of Excellence for Power System Automation and Operation, Iran Univ. of Science and Technology
2- Department of Automatic Control and Industrial Informatics, Technical University of Catalonia, Spain
3- Department of Energy Technology, Aalborg University, Denmark
4- Department of Electrical Engineering, National Sun Yat-sen University, Taiwan
savaghebi@iust.ac.ir

Abstract: *In this paper, a method for voltage harmonic compensation in a microgrid operating in islanded and grid-connected modes is presented. Harmonic compensation is done through proper control of distributed generators (DGs) interface converters. In order to achieve proper sharing of the compensation effort among the DGs, a power named "Harmonic Distortion Power (HDP)" is defined. In the proposed method, the active and reactive power control loops are considered to control the powers injected by the DGs. Also, a virtual impedance loop and voltage and current proportional-resonant controllers are included. Simulation results show the effectiveness of the proposed method for compensation of voltage harmonics to an acceptable level.*

Keywords: Distributed Generation (DG), Microgrid (MG), voltage harmonic compensation, grid-connected, islanded.

1. Introduction

Distributed Generators (DGs) may be connected individually to the utility grid or be integrated to form a local grid which is called microgrid (MG). The MG can operate in grid-connected (connected to the utility grid) or islanded (isolated from the utility grid) modes [1]. DGs often consist of a prime mover connected through an interface converter (e.g. an inverter in the case of dc-to-ac conversion) to the power distribution system (microgrid or utility grid). The main role of this inverter is to control voltage amplitude and phase angle in order to inject the active and reactive powers. In addition, compensation of power quality problems, such as voltage harmonics can be achieved through proper control strategies.

In [2]-[4], some approaches are presented to use DG for voltage harmonic compensation.

A single-phase DG capable of improving voltage waveform is presented in [2]. For voltage harmonic compensation, DG is controlled to operate as a shunt active power filter. In the other words, DG injects harmonic current to improve voltage waveform.

The approach of [3] is based on making the output voltage of the DG nonsinusoidal in a way that after voltage drop on the distribution line, voltage waveform at the point of common coupling (PCC) becomes sinusoidal. This approach is effective for PCC voltage improvement, but, its negative effect on the power control of DG is not analyzed.

An approach for compensation of voltage harmonics in an islanded MG is presented in [4]. In this approach which is implemented in the synchronous (dq) reference frame, DGs are controlled to absorb harmonic current of the load like a shunt active filter. Also, the method of harmonic compensation effort sharing among the DGs is presented.

In this paper, the approach of [4] is extended to be applicable for both grid-connected and islanded modes of microgrid operation. On the other hand, the method of compensation effort sharing is improved. In the proposed method, the overall control system is designed in the stationary ($\alpha\beta$) reference frame.

The control structure consists of the following loops: active and reactive power controllers, virtual impedance loop, voltage and current controllers, and voltage harmonic compensator. The details are provided in the next Section.

2. DG Inverter Control Strategy

Fig. 1 shows the power stage of the utility grid and the MG formed by two DGs. The MG consists of a DC prime mover, an inverter, a LC filter for each DG and also an inductor between each DG and the load connection point which models the distribution line. As it can be seen in this Fig., a three-phase diode rectifier is considered as the nonlinear load.

Also, a static switch is considered to connect/disconnect the MG to/from the utility grid (grid-connected/islanded operation). A distribution line shown as a resistance (R_g) in series with an inductance (L_g) is considered between MG and the utility grid.

The proposed control strategy for the DG inverter is also shown in Fig. 1. All the control loops of this Fig. are in $\alpha\beta$ reference frame. The Clarke transformation is used to transform the variables between abc and $\alpha\beta$ frames. The control system details are as follow.

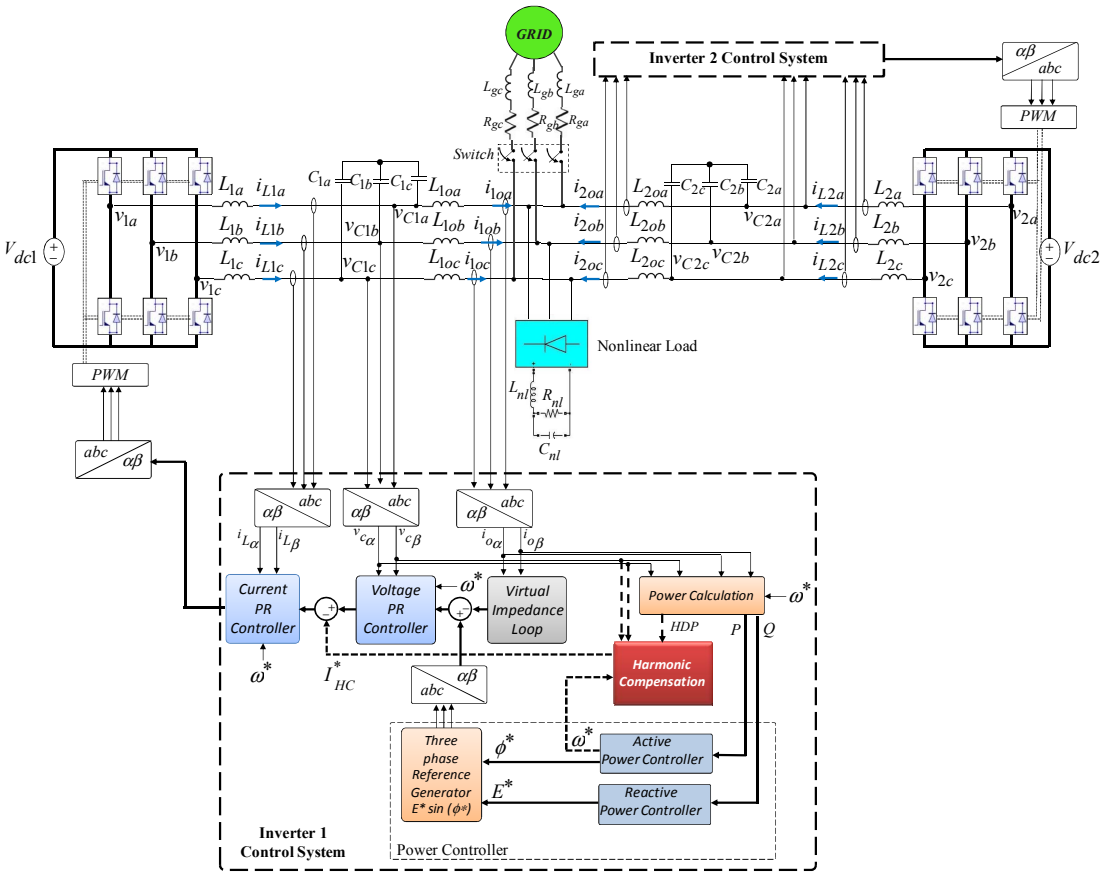

Fig. 1: Power stage and the control system of a MG operating in grid-connected or islanded mode

2.1 Power Calculation

As shown in Fig. 1, $\alpha\beta$ components of the DG output voltage ($v_{c\alpha}$ and $v_{c\beta}$) and output current ($i_{o\alpha}$ and $i_{o\beta}$) are fed to "*Power Calculation*" block. Then, the active and reactive powers at fundamental frequency (P and Q, respectively) and "*Harmonic Distortion Power (HDP)*" are calculated. The details are as follow.

2.1.1. Fundamental Active and Reactive Powers

The instantaneous values of active and reactive powers are calculated by using the following equations [5]:

$$p = v_{c\alpha}\, i_{o\alpha} + v_{c\beta}\, i_{o\beta} \tag{1}$$

$$q = v_{c\beta}\, i_{o\alpha} - v_{c\alpha}\, i_{o\beta} \tag{2}$$

Then, the dc components of p and q (P and Q) (which are the fundamental active and reactive powers, respectively) are extracted by using two first-order low pass filters with the cut-off frequency of 2Hz.

2.1.2. Harmonic Distortion Power

In this paper, a power named as "*Harmonic Distortion Power (HDP)*" is used for sharing of harmonic compensation effort. This power is defined as follows:

$$HDP = 3 * V_{harm,rms} * I_{harm,rms} \tag{3}$$

In equation (3), $V_{harm,rms}$ and $I_{harm,rms}$ are the RMS values of the harmonic (oscillatory) component of DG output voltage and current, respectively.

In order to calculate RMS values, at first, the fundamental component of output voltage and current is extracted and then, subtracted from the total (including both fundamental and oscillatory components) output voltage and current, respectively. At last, the RMS of the resultant values is calculated.

For extraction of fundamental component of output voltage and current, second-order generalized integrators (SOGIs) [6] are used. The SOGI diagram is shown in Fig. 2(a), where ω is the SOGI resonant frequency. A SOGI-based second-order bandpass filter (BPF), for the extraction of fundamental component, with the following transfer function can be achieved as shown in Fig. 2(b).

$$BPF(s) = \frac{X_{j,1}(s)}{X_j(s)} = \frac{k\omega^* s}{s^2 + k\omega^* s + (\omega^*)^2} \tag{4}$$

where

- X: voltage or current
- j and 1: subscripts represent α or β and fundamental component, respectively
- ω^*: reference frequency of the microgrid
- k: a constant which determines the BPF bandwidth

With the decrease of k, BPF becomes more selective but slower [6]. In this paper, k is set to $2\sqrt{2}$.

2.2 Active and Reactive Power Control

Assuming a DG which is connected to the electrical network through a mainly inductive distribution line, P and Q can be approximated as follows [7], [8]:

$$P = \frac{EV}{X}\phi \tag{5}$$

$$Q = \frac{V}{X}(E - V) \tag{6}$$

where E is the magnitude of the inverter output voltage, V is the network bus voltage magnitude, ϕ is the load angle (the angle between E and V), and X is the distribution line reactance. Considering the phase angle of the network voltage to be zero, ϕ will be equal to the inverter voltage phase angle.

Thus, the active and reactive powers can be controlled by the DG output voltage phase and amplitude, respectively. According to this, the following droop characteristics [9] are considered to control active and reactive powers of DGs in a MG.

$$\phi^* = \phi_0 + m_P(P_{ref} - P) + m_I\int(P_{ref} - P) \tag{7}$$

$$E^* = E_0 + n_P(Q_{ref} - Q) + n_I\int(Q_{ref} - Q) \tag{8}$$

where

- E^* : voltage amplitude reference
- ϕ^* : phase angle reference
- E_0 : rated voltage amplitude
- ϕ_0 : rated phase angle ($\int \omega_0 dt$)
- ω_0: rated angular frequency
- m_P : active power proportional coefficient
- m_I : active power integral coefficient
- n_P : reactive power proportional coefficient
- n_I : reactive power integral coefficient

In the islanded operation of MG, P_{ref} and Q_{ref} must be set to zero, because, in this mode *DGs* are the only sources of supplying the loads. In the other words, load imposes its required power to the DGs. Also, in this mode n_I must be zero, because, if the controllers try to share Q exactly (zero steady-state error through integral term), voltage becomes instable [9].

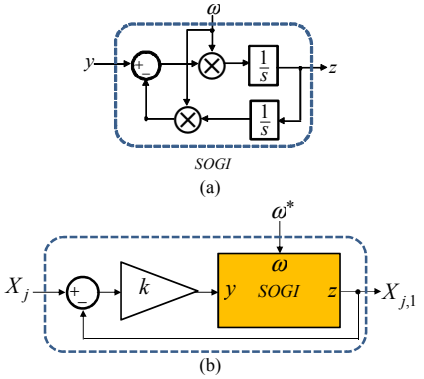

Fig. 2: (a) SOGI structure (b) BPF block diagram

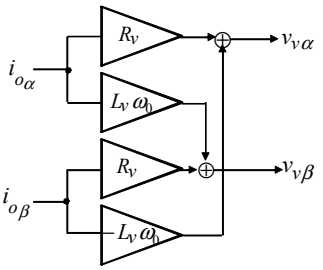

Fig. 3: Virtual impedance block diagram

But, m_I may have nonzero value in both islanded and grid-connected modes. In the islanded mode, equation (7) acts as a proportional-derivative controller for frequency. The derivative term (m_p) improves the dynamic behavior of the microgrid [7].

In the grid-connected mode, load is supplied by the DGs and the utility grid. In this mode, equations (7) and (8) act as Proportional-Resonant (PI) controllers which make the P and Q track the specified references.

2.3 Virtual Impedance Loop

Addition of the virtual resistance control loop makes the oscillations of the system more damped [7]. Also, virtual inductance is considered to ensure the decoupling of P and Q. Thus, virtual impedance makes the droop controller more stable [10].

The virtual impedance can be achieved as shown in Fig. 3, where R_v and L_v are the virtual resistance and inductance values, respectively [11]. As it can be seen in Fig. 3, the rated frequency (ω_0) is used in this loop, since it has very low difference with operating frequency. Also, a fixed value is preferable to avoid undesirable interactions among the control loops which could lead to instability.

2.4 Voltage and Current Proportional-Resonant (PR) Controllers

Proportional-resonant (PR) controllers are often used in the stationary reference frame control systems [12]. In this paper, voltage and current PR controllers are as follow

$$G_V(s) = k_{pV} + \frac{2k_{rV}\omega_c s}{s^2 + 2\omega_c s + (\omega^*)^2} \tag{9}$$

$$G_I(s) = k_{pI} + \frac{k_{rI1}\,s}{s^2 + (\omega^*)^2} + \frac{k_{rI5}\,s}{s^2 + (5\omega^*)^2} + \frac{k_{rI7}\,s}{s^2 + (7\omega^*)^2} \tag{10}$$

where

- k_{pV} : voltage proportional coefficient
- k_{rV} : voltage resonant coefficient
- ω_c : voltage central frequency
- k_{pI} : current proportional coefficient
- k_{rI1} : current resonant coefficient at fundamental frequency

- k_{rI5}: current resonant coefficient at 5th harmonic
- k_{rI7}: current resonant coefficient at 7th harmonic

As shown in Fig. 1, the voltage controller follows the mainly fundamental frequency reference which is generated by the virtual impedance loop and the droop characteristics. So, only the fundamental frequency resonant controller is considered. Also, to achieve more stability, the resonant part is considered as a BPF. [13].

Furthermore, since the "*Harmonic Compensation*" block output contains harmonic components (as described in the next Subsection), the resonant parts for the main harmonics (5th and 7th) are included in the current controller.

Considering the parameters listed in TABLE I, the Bode diagrams of voltage and current controllers are as Figs. 4(a) and 4(b), respectively.

As shown, current controllers provide very high gain at 1st (fundamental), 5th, and 7th harmonics which provides zero steady-state error.

Also, voltage controller has a wider resonant peak, therefore is less sensitive to frequency fluctuations. The gain at resonant frequency is limited, however, still high enough to ensure a small tracking error.

Finally, as shown in Fig.1, the output of the current controller is transformed back to the *abc* frame to provide the reference three-phase voltage for the pulse width modulator (*PWM*). The *PWM* block controls the switching of the DG inverter.

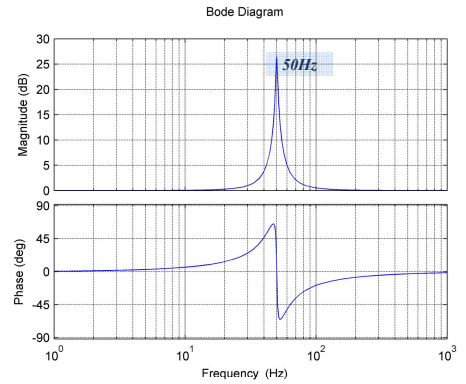

(a)

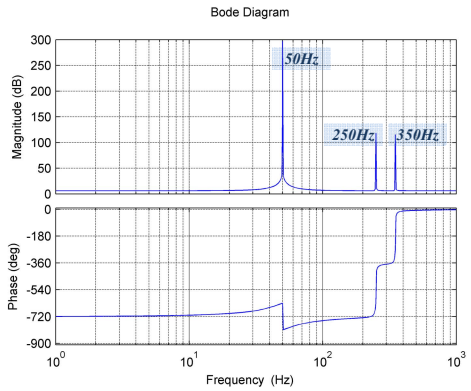

(b)

Fig. 4: Bode diagrams: (a) voltage controller (b) current controller

2.5 Voltage Harmonics Compensation

In this paper, the harmonic compensation method of [4] is improved in terms of harmonic compensation effort sharing. Also, the approach presented here is applied for both grid-connected and islanded modes of MG operation.

The details of "*Harmonic Compensation*" block of Fig. 1 are shown in Fig. 5. As seen, at first, the fundamental component of the DG output (capacitor) voltage is extracted using a SOGI-based BPF (Fig. 2(b)) tuned at fundamental frequency. Then, the voltage harmonics (oscillatory voltage: $v_{harm.}$) is extracted by subtracting the fundamental part from the DG output voltage. On the other hand, *HPD* is multiplied by a constant which is called "*Harmonic Compensation Gain (HCG)*" to generate "*Harmonic Conductance Command (G*)*". Thus, the amount of compensation is proportional to *HDP* and *HCG*. Proper selection of *HCG* ensures that the compensation will not lead to DG inverter overloading or control system instability. Finally, $v_{harm.}$ and *G** are multiplied to generate harmonic compensation reference current (I^*_{HC}). In this way, *G** makes the DG behave as a resistance at harmonic frequencies to damp the voltage harmonics.

As a result of compensation, *HDP* will decrease (as presented in the next Section). So, an inherent negative feedback exists in this compensation method. This is like a droop characteristics which helps to achieve sharing of compensation effort.

On the other hand, in [4] a power named "*Harmonic Volt-Ampere Reactive (H)*" is used for sharing of harmonic compensation effort among the DGs. With the compensation of voltage harmonics this power increases. So, in order to achieve sharing of compensation effort, the following droop characteristic is used in [4].

$$G^* = G_0 + HCG(H_0 - H) \tag{11}$$

In (11), H_0 and G_0 are the rated values of harmonic VAr and conductance, respectively.

The method presented in [4] for estimation of H_0 is not straight-forward. Furthermore, if $H>H_0$ the control system becomes instable. Also, inclusion of G_0 in (11) is not justified in [4]. In the present paper, these problems are solved through using *HDP* instead of *H* for sharing of harmonic compensation effort.

3. Simulation Results

Simulation studies are performed on the electrical system of Fig. 1. The MG and the utility grid are rated at 400V/50Hz. Other power stage parameters are presented in TABLE II. For simplicity, *a*, *b* and *c* subscripts are not shown in this TABLE, since the electrical system is balanced. In order to simulate

asymmetrical distribution lines, $L_{1o}=L_o/2$ and $L_{2o}=L_o$. The switching frequency of the DGs inverter is 10 kHz.

R_v and L_v are chosen as 1Ω and 2mH, respectively. The parameters of the power controllers are listed in TABLE III. As mentioned earlier, in the islanded mode n_I is zero.

HCG is set to 0.0145 and 0.0120 for islanded and grid-connected modes, respectively. Harmonic compensation is activated at t=0.6sec. In order to avoid control system oscillations, compensation is activated by multiplying I^*_{HC} with a ramp having the rise-time of 0.05sec.

3.1 Islanded Operation

As mentioned before, in the islanded mode $P_{ref}=0$ and $Q_{ref}=0$. In this way, the power controllers will act to achieve even sharing of *P* and *Q* between the DGs.

Fig. 6 shows *P* and *Q* sharing of the DGs. It can be seen that in spite of unequal line impedance between DGs and the nonlinear load connection point, the powers are well-shared and the well-sharing is maintained after harmonic compensation activation.

DGs output voltage improvement after compensation activation is obvious in Fig. 7. As seen, DG1 output voltage is more distorted, since the line impedance between DG1 and the nonlinear load connection point is lower. DGs output voltage *THD* and *HDP* are shown in Figs. 8(a) and 8(b), respectively. As shown, as a result of compensation *THD* and *HDP* values are significantly decreased.

3.2 Grid-Connected Operation

In the grid-connected mode, $P_{ref}=1500$, $Q_{ref}=0$. P_{ref} is applied at t=0.4sec by multiplying with a ramp. The ramp rise-time is 0.1sec. It is noteworthy that in grid-connected mode, Q_{ref} may have other non-zero values.

Fig. 9 shows *P* and *Q* of two DGs. It can be seen that the reference values are tracked well. Also, utility grid active and reactive powers (P_g and Q_g, respectively) are shown in Fig. 10.

DGs output voltages can be seen in Fig.11. DGs voltage *THD* and *HDP* which shown in Figs. 12(a) and 12(b), respectively, are decreased due to compensation.

TABLE I: PR Controllers Parameters

k_{pV}	k_{rV}	ω_c	k_{pI}	k_{rI1}	k_{rI5}	k_{rI7}
1	20	4	2	500	90	90

TABLE II: Electrical System Parameters

V_{dc} (V)	L (mH)	C (μF)	L_o (mH)	R_{nl} (Ω)	L_{nl} (mH)	C_{nl} (μF)	R_g (Ω)	L_g (mH)
650	1.8	25	1.8	25	0.084	235	0.5	5

TABLE III: Power Controllers Parameters

E_0	ω_0	m_P	m_I	n_P	n_I
$230\sqrt{2}$	100pi	0.0002	0.0015	0.015	0.3

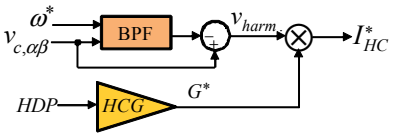

Fig. 5: Block diagram of voltage harmonic compensation

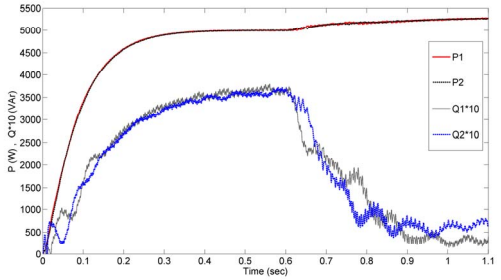

Fig. 6: *P* and *Q* sharing (islanded mode)

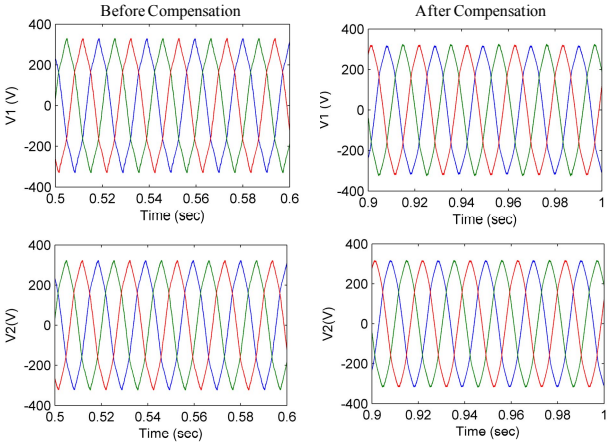

Fig. 7: DGs output voltage waveforms (islanded mode)

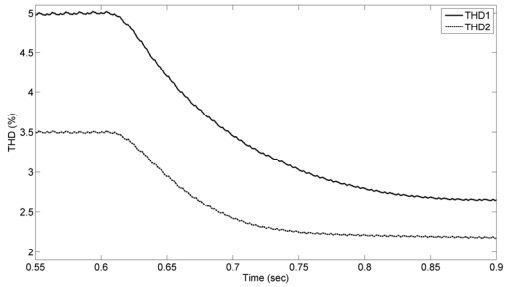

(a)

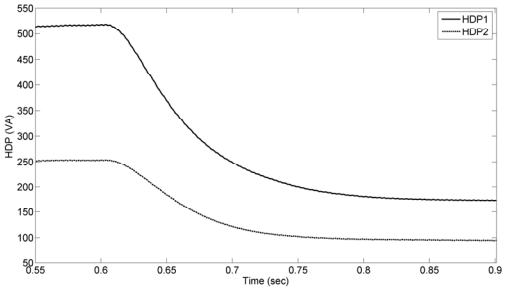

(b)

Fig. 8: (a) *THD* (b) *HDP* (islanded mode)

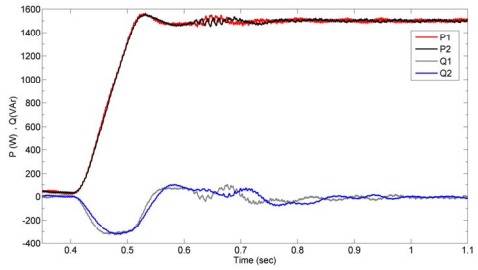

Fig. 9: *P* and *Q* of two DGs (grid-connected mode)

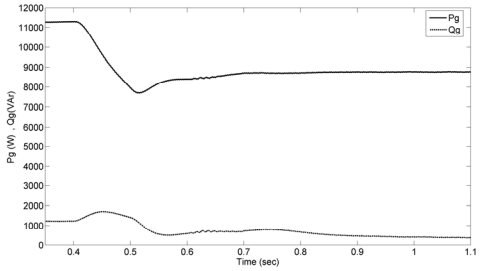

Fig. 10: Utility grid active and reactive powers

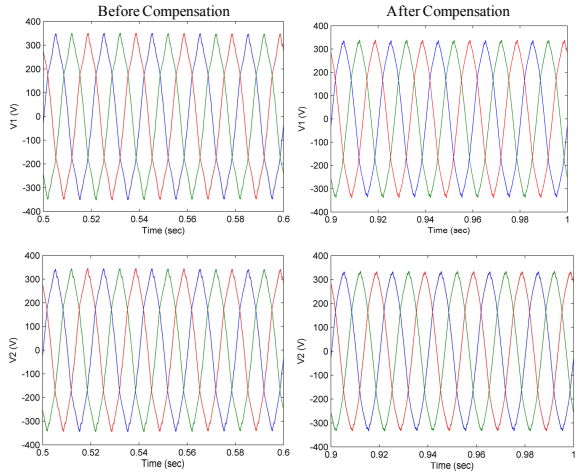

Fig. 11: DGs output voltage waveforms (grid-connected mode)

4. Conclusions

In this paper, an approach for compensation of voltage harmonics in a microgrid operating in islanded and grid-connected modes is presented. In order to improve sharing of harmonic compensation effort, a new definition for harmonic distortion power is used.

The results show that by using the proposed control approach fundamental and harmonic distortion powers are properly shared between DGs and also the output voltage waveforms are improved.

References

[1] S. B. Patra, "Techniques for developing reliability-oriented optimal microgrid architectures," PhD. Diss., New Mexico State University, May 2007.

[2] M. Cirrincione, M. Pucci, and G. Vitale, "A single-phase DG generation unit with shunt active power filter capability by adaptive neural filtering," IEEE Trans. Ind. Elec., vol. 55, no. 5, pp. 2093-2110, May 2008.

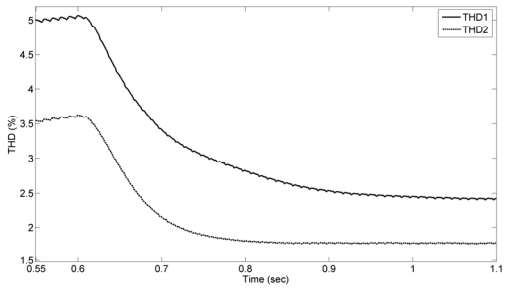

(a)

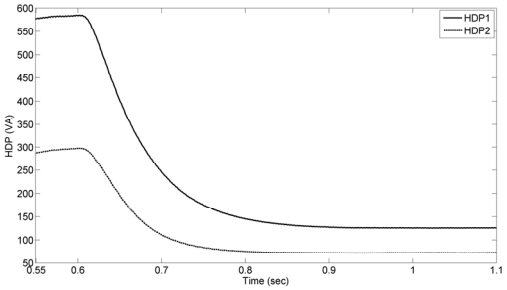

(b)

Fig. 12: (a) *THD* (b) *HDP* (grid-connected mode)

[3] H. Patel, and V. Agarwal, "Control of a stand-alone inverter-based distributed generation source for voltage regulation and harmonic compensation," IEEE Trans. Pow. Del., vol. 23, no. 2, pp. 1113-1120, Apr. 2008.

[4] T. L. Lee, and P. T. Cheng, "Design of a new cooperative harmonic filtering strategy for distributed generation interface converters in an islanding network," IEEE Trans. Pow. Elec., vol. 22, no. 5, pp. 1919-1927, Sept. 2007.

[5] H. Akagi, Y. Kanagawa, and A. Nabase, "Instantaneous reactive power compensator comprising switching devices without energy storage components," IEEE Trans. Ind. App., vol. IA-20, no. 3, p. 625, May/Jun. 1984.

[6] M. Ciobotaru, R. Teodorescu, and F. Blaabjerg, "A new single-phase PLL structure based on second order generalized integrator," Pow. Elec. Specialists Conf. (PESC), Oct. 2006.

[7] J. M. Guerrero, J. Matas and L. G. de Vicuña, M. Castilla, and J. Miret, "Decentralized control for parallel operation of distributed generation inverters using resistive output impedance," IEEE Trans. Ind. Elec., vol. 54, no. 2, pp. 994-1004, Apr. 2007.

[8] E. Barklund, N. Pogaku, M. Prodanovic´, C. Hernandez-Aramburo, and T. C. Green, "Energy management in autonomous microgrid using stability-constrained droop control of inverters," IEEE Trans. Pow. Elec., vol. 23, no. 5, pp. 2346-2352, Sept. 2008.

[9] Y. Li, D. M. Vilathgamuwa, and P. C. Loh, "Design, analysis, and real-time testing of a controller for multibus microgrid system," IEEE Trans. Pow. Elec., vol. 19, no. 5, pp. 1195-1204, Sept. 2004.

[10] J. M. Guerrero, L. G. Vicuna, J. Matas, M. Castilla, and J. Miret, "Output impedance design of parallel-connected UPS inverters with wireless load sharing control," IEEE Trans. Ind. Elec., vol. 52, no. 4, pp. 1126-1135, Aug. 2005.

[11] J. He, and Y. W. Li "Analysis and design of interfacing inverter output virtual impedance in a low voltage microgrid," Energy Conv. Cong. and Exp. (ECCE) proc., pp. 2857–2864, 2010.

[12] F. Blaabjerg, R. Teodorescu, M. Liserre, and A. V. Timbus, "Overview of control and grid synchronization for distributed power generation systems," IEEE Trans. Ind. Elec., vol. 53, no. 5, pp. 1398-1409, Oct. 2006.

[13] Y. Li, D. M. Vilathgamuwa, and P. C. Loh, "Microgrid power quality enhancement using a three-phase four-wire grid-interfacing compensator", IEEE Trans. Ind. Appli., vol. 41, no. 6, pp. 1707-1719, Nov./Dec. 2005.